



# Low phase noise operation of a cavity-stabilized 698 nm AlGaInP-based VECSEL

PAULO HISAO MORIYA, \*  MARTIN LEE,   
AND JENNIFER E. HASTIE 

*Institute of Photonics, Department of Physics, SUPA, University of Strathclyde, 99 George Street, Glasgow G1 1RD, UK*

\*[paulo.moriya@strath.ac.uk](mailto:paulo.moriya@strath.ac.uk)

**Abstract:** We report for the first time a high performance, single frequency AlGaInP-based VECSEL (vertical-external-cavity surface-emitting-laser) with emission at 698 nm, targeting the clock transition of neutral strontium atoms. Furthermore, we present comprehensive noise characterization of this class-A semiconductor laser, including the residual fast phase noise in addition to the frequency and relative intensity noise. The low noise VECSEL has output power at around 135 mW with an estimated linewidth of 115 Hz when frequency stabilized via the Pound-Drever-Hall (PDH) technique to a high finesse reference cavity, without intermediate stabilization. The phase noise is measured to be below  $-126$  dBc/Hz for frequencies between 10 kHz and 15 MHz with a total integrated phase noise of 3.2 mrad, suitable not only for ultra-cold neutral strontium-based quantum technologies, such as optical clocks, but also with potential for atom-interferometry applications.

Published by Optica Publishing Group under the terms of the [Creative Commons Attribution 4.0 License](https://creativecommons.org/licenses/by/4.0/). Further distribution of this work must maintain attribution to the author(s) and the published article's title, journal citation, and DOI.

## 1. Introduction

Laser systems with high spatial and spectral brightness, stability, and tunability at visible wavelengths are critical for quantum matter creation and manipulation [1], and precise optical measurements such as those required for optical clocks [2,3], atom interferometers [4], high resolution spectroscopy [5], coherent light detection and ranging (LIDAR) [6] and fiber sensing [7]. Ultra-narrow linewidths usually require active stabilization to a robust frequency reference, such as an optical resonator, in order to counteract spectral broadening above the intrinsic linewidth limit [8,9] caused by external factors, such as the environment, pump lasers, and electronics. The extra noise contributes to two distinct regions of the laser noise spectrum; at low and high Fourier frequencies separated by the so-called  $\beta$ -separation line [10]. The former is related to slow frequency noise/large phase noise which contributes to the narrow central part of the laser spectrum, or laser linewidth. The latter is related to fast frequency noise/small phase noise which contributes to the wings (or pedestal) of the spectrum, with no contribution to the laser linewidth [10,11]. External cavity diode lasers (ECDLs) are commonly employed in quantum technology systems but present significant residual phase noise at high frequencies, beyond the correction bandwidth of the stabilization system [11,12], which can affect the stability and precision of gravimeters and gradiometers based on cold atom interferometry [4]. Other laser technologies, such as those based on stimulated Brillouin scattering (SBS) [13] and self-injection locking (SIL) [14,15], are emerging as more integrable solutions for similar applications [16], but the former still requires a separate pump laser, and emission at visible wavelengths remains challenging, particularly for output power of more than a few mW.

Alternatively, vertical-external-cavity surface-emitting-lasers (VECSELs) [17] are being investigated for cold-atom-based quantum technology applications where high performance in output power, beam quality, stability and noise is crucial. VECSELs present class-A carrier

dynamics, thanks to short gain lifetimes, very low spontaneous emission factors, and high finesse resonators, resulting in ultra-low noise performance with a mHz-level intrinsic linewidth, or Schawlow-Townes-Henry limit [8,9]. Another important feature of VECSELs is the possibility of tailoring the emission wavelength through compound semiconductor bandgap engineering without the need for doping [17], increasing wavelength coverage. The latter is also an important feature for cold-atoms applications where multiple laser systems with a narrow range of wavelengths are exploited as, for example, for neutral strontium atoms used for optical clocks [18]. Neutral Sr atoms combine triplet states with re-pump transitions requiring multiple laser systems, each with different linewidth requirements at 689, 698, and 679 and 707 nm [19] for the second-stage laser cooling, clock, and re-pump transitions, respectively. Recently, our group has demonstrated sub-kHz linewidth operation of GaInP/AlGaInP-based VECSELs with emission at 689 nm, pumped by a commercial green semiconductor laser in the first case [20], and latterly by a blue InGaN diode laser [21]. Output power exceeding 150 mW was achieved in both cases, and linewidths of 200 Hz and 570 Hz, respectively, meeting requirements for the second cooling transition of neutral strontium atoms used for the development of quantum technologies. Although frequency and intensity noise have been extensively investigated, characterization of the phase noise performance of single-frequency VECSELs is usually reported as part of the laser linewidth or intensity noise, given that both are correlated via the Henry factor [22]; however, we note previous reports of phase noise characterization of the *beat note* of dual frequency VECSELs, or DF-VECSELs (see e.g. [22–25]), and timing jitter of mode-locked VECSELs [26]. Previous work on DF-VECSEL noise performance characterization also includes extensive theoretical studies to calculate *free-running* behavior based on laser parameters, and the coupling and correlation between the two modes [22–24], with single frequency performance estimated if the modes are uncoupled and uncorrelated. The phase noise spectrum of DF-VECSELs is dominated by semiconductor gain structure thermal fluctuations and technical noise at low frequencies and by the Henry factor at high frequencies [22–25]. Although these theoretical results are useful to predict the single frequency VECSEL noise performance, experimental characterization when free-running or cavity-locked is of particular interest to demonstrate the suitability for applications requiring single frequency lasers with ultra-low phase noise. These include atom interferometers [4,27], coherent LIDAR [6], and spectroscopy [5], where excessive laser phase noise can be amplified by other parts of the optical setup or decrease the efficiency and accuracy of measurements, thus increasing the optical power requirements.

Here, we report for the first time a 698 nm VECSEL, developed to target the clock transition of neutral strontium atoms, achieving output powers exceeding 130 mW with estimated linewidth of 115 Hz. In addition to frequency and relative intensity noise, the residual fast phase noise is characterized when the VECSEL system is locked to an ultra-high finesse cavity, using the measurement method recently reported by Schmid et al [11]. The phase noise of the VECSEL is  $< -126$  dBc/Hz for frequencies above 10 kHz, which is 10 dB lower than that reported for dual frequency VECSEL systems [25]. Furthermore, this represents a reduction of at least 5 dB when compared to ECDL counterparts that require extra noise cancellation setups [4], thus also helping to reduce the overall laser system bulkiness and complexity.

## 2. Narrow linewidth VECSEL system

### 2.1. VECSEL set-up

The GaInP/AlGaInP-based VECSEL gain structure is similar to those previously reported by our group [20] for emission at around 690 nm when optically-pumped at green wavelengths around 532 nm (see Fig. 1(a)). The active region is formed by 16 compressively-strained GaInP quantum wells (QWs), grouped in pairs at optical field antinodes, separated by AlGaInP barriers and grown on top of an AlGaAs/AlAs distributed Bragg reflector (DBR) mirror on a GaAs substrate. A  $4 \times 4$  mm<sup>2</sup> gain structure sample is capillary-bonded to an uncoated 500- $\mu$ m-thick, optical grade,

low birefringence ( $\Delta n < 10^{-6}$ ) synthetic diamond heat-spreader [28]. The composite sample is kept in a brass mount, temperature-stabilized via thermo-electric cooling (stability = 0.01 °C).

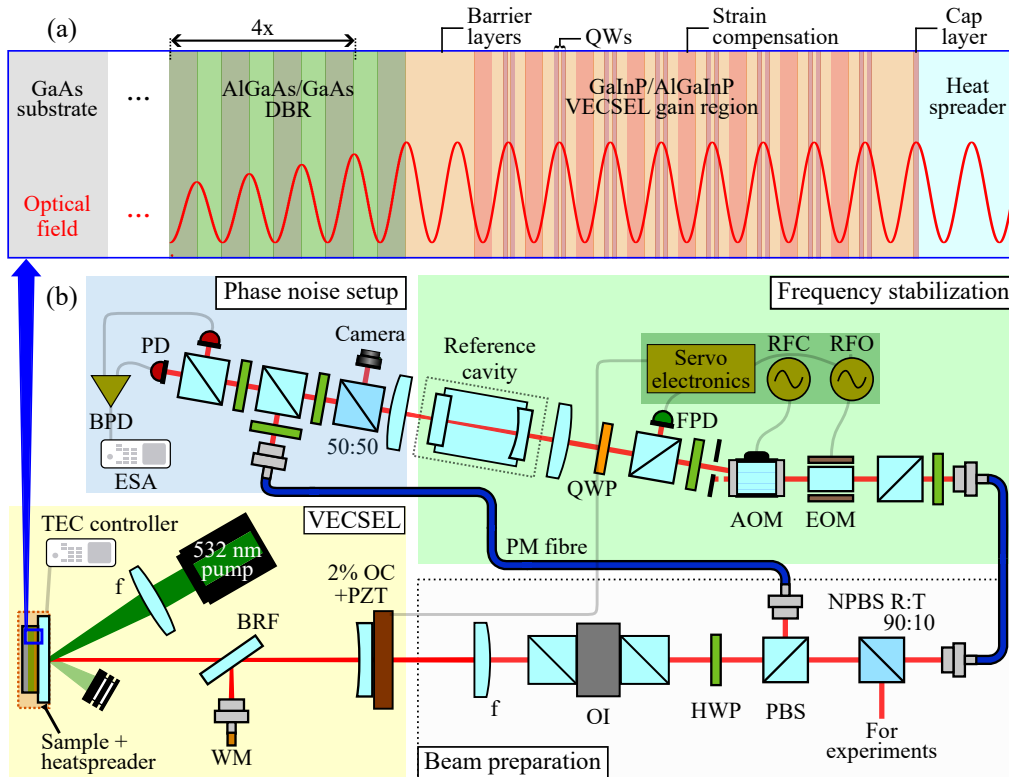


**Fig. 1.** (a) Schematic of the AlGaInP-based VECSEL gain structure for laser oscillation at 698 nm. (b) Schematic of the optical set-up including: AlGaInP-based VECSEL (yellow box); Pound-Drever-Hall frequency stabilization (green box); and phase noise characterization (blue box). QWs: quantum wells; DBR: distributed Bragg reflector; TEC: thermo-electric cooling; f: lens; BRF: birefringent filter; OC: output coupler; PZT: piezo electric transducer; OI: optical isolator; WM: wavemeter; H(Q)WP: half(quarter)-wave plate; PBS: polarizing beam splitter; NPBS: non-polarizing beam splitter; R: reflection; T: transmission; PM fibre: polarization maintaining fibre; AOM: acousto-optic modulator; RFC: radio-frequency controller; EOM: electro-optic modulator; FPD: fast photodiode; PD: photodiode; RFO: radio frequency oscillator; BPD: balanced photodetector; ESA: electrical spectrum analyzer.

A linear, or two-mirror, laser cavity is built (see Fig. 1(b), yellow box), consisting of the sample DBR and a 2% transmission, plano-concave output coupler ( $\varnothing = 6$  mm, thickness = 3 mm and radius of curvature = 100 mm) mounted on a piezo-electric transducer (PZT) for frequency stabilization purposes. Laser oscillation is achieved when the gain structure is optically pumped at 532 nm with pump power up to 3.5 W by a commercial optically-pumped semiconductor laser (OPSL, Coherent Verdi G5). Multimode output power of 240 mW at wavelengths around 695 nm is achieved with slope efficiency of 10.3% and threshold of 0.91 W. Single frequency operation is achieved by inserting an intra-cavity birefringent filter (BRF) at Brewster's angle (quartz plate, thickness = 4 mm), and optimization of laser cavity length and alignment. In this regime, slope efficiency is reduced to 5.7% and output power exceeding 130 mW is achieved at 698 nm with free-running linewidth of  $(130 \pm 20)$  kHz (see Fig. 2(a) *inset*). Wavelength tunability is achieved via control of the sample temperature for fine tuning with sub-pm precision [29], and rotation of

the BRF for coarse tuning, ranging from 692 to 702 nm at sample mount temperature of 18 °C and from 694 nm to 703 nm at 24 °C (see Fig. 2(a)).

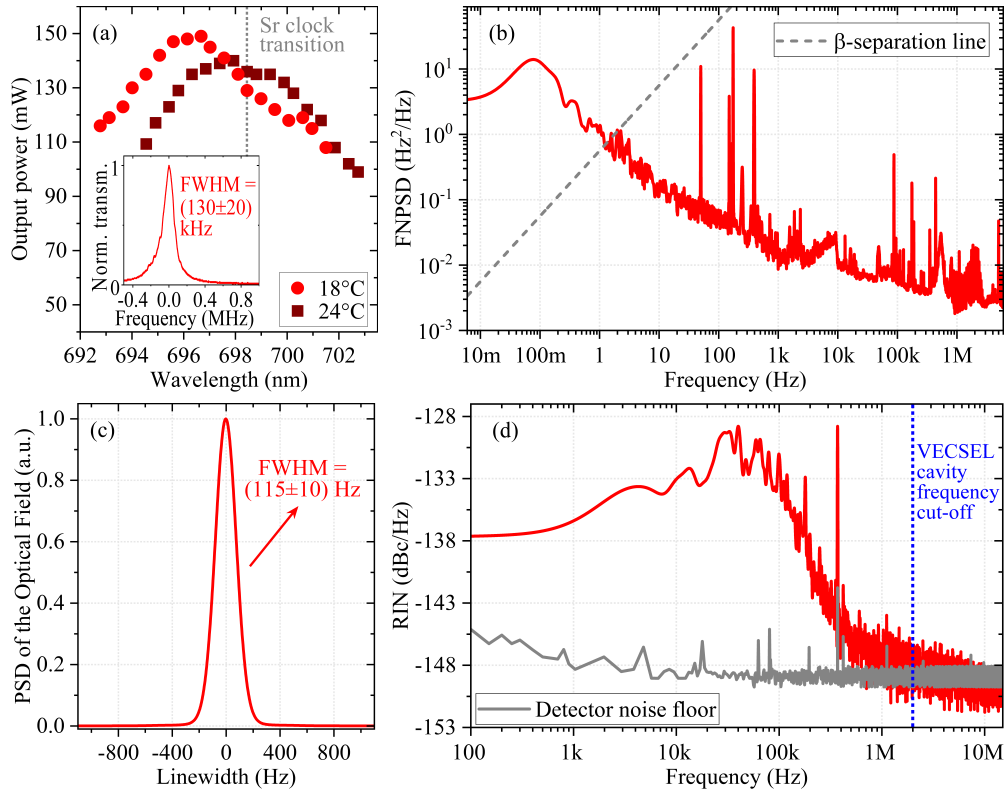


**Fig. 2.** (a) Emission wavelength tuning curves via BRF rotation for VECSEL sample mount temperature of 18 and 24 °C. *inset:* Free-running linewidth measured from the spectrum transmitted by the reference cavity (normalized). (b) Frequency noise power spectral density of the GaInP/AlGaInP-based VECSEL when actively-stabilized via the PDH technique. The  $\beta$ -separation line (dash line) is also plotted, dividing the graph into two regions with low and high frequency modulation, which contribute to the central peak and wings of the laser line-shape, respectively. (c) Power spectral density of the optical field of the locked VECSEL, reconstructed via autocorrelation and the Wiener-Khinchine theorem from the spectrum presented in (c). A linewidth of  $(115 \pm 10)$  Hz is estimated. (d) Relative intensity noise (RIN) of the locked GaInP/AlGaInP-based VECSEL at 698 nm, measured with a detector bandwidth of 11 MHz.

## 2.2. Frequency and intensity noise analysis

Frequency stabilization of the laser resonator is implemented via the PZT on which the laser output coupler is mounted, using the Pound-Drever-Hall (PDH) technique [30] (see Fig. 1, green box). For this purpose, 10% of the VECSEL output power is picked off and sent to the frequency stabilization setup via a polarization maintaining optical fibre. The laser light is then frequency modulated by an electro-optic modulator (EOM; FM = 74 MHz) and shifted by an acousto-optic modulator (AOM; FM = 100 MHz) then coupled to a 100-mm-long reference cavity made of ultra-low expansion (ULE) glass. The photon lifetime (relative to the drop of transmitted power) is measured via cavity ring-down spectroscopy [22] to be 30.3  $\mu$ s, corresponding to a full width at half maximum (FWHM) linewidth of 5.2 kHz and an estimated finesse of 288 k for a free

spectral range (FSR) of 1.5 GHz. The VECSEL performance when locked was first investigated in terms of frequency and relative intensity noise.

Frequency noise is analyzed by the power spectral density (PSD, see Fig. 2(b)), calculated via the residual AC error signal from the servo controller recorded over acquisition times of 100s. Similar to other breadboard systems, thermal and environmental noise along with pump noise are the major components of the VECSEL frequency noise. Injection of noise into the VECSEL cavity is filtered first by its external cavity which acts as a low-pass filter with a cut-off frequency of 2 MHz, then further reduced by the active frequency stabilization implemented (bandwidth = 30 kHz). Figure 2(b) also shows the  $\beta$ -separation line, defined as  $S_{\beta}(f) = 8(\ln 2)f/\pi^2$  [10], where  $f$  is Fourier frequency, which divides the frequency noise contributions to the laser line-shape: the central (Gaussian) component, affecting directly the linewidth, and the wings (Lorentzian), for  $S_{\beta}(f) < S_v(f)$  and  $S_{\beta}(f) > S_v(f)$ , respectively. Furthermore, using auto-correlation and the Wiener-Khintchine theorem [10], a linewidth of  $(115 \pm 10)$  Hz (see Fig. 2(c)) is estimated from the PSD by reconstructing the shape of the optical field, similar to linewidths previously reported by our group [20,21]. The frequency noise and, consequently, linewidth results presented here are limited by thermal and mechanical instabilities affecting both the reference and VECSEL cavity, as it was not placed in a housing under ultra-high vacuum. Furthermore, pump intensity stabilization would also help to reduce the injection of noise into the VECSEL system thus helping to get closer to the ultra-narrow intrinsic linewidth of VECSEL.

Figure 2(d) shows the locked 698 nm VECSEL relative intensity noise (RIN) measurement. Pump laser intensity noise, contributing to all frequencies up to the VECSEL cavity cut-off, in addition to mechanical and thermal ( $f < 1$  kHz), and electronic noise not suppressed by the active stabilization implemented to the VECSEL are responsible for the majority of the VECSEL RIN. The RIN is measured to be  $< -129$  dBc/Hz for all frequencies in the range presented here and  $< -140$  dBc/Hz for  $f > 350$  kHz, above the detector noise floor for frequencies below 7 MHz.

### 3. Phase noise measurements

The residual fast phase noise measurement (see blue box, Fig. 1) was built alongside the frequency stabilization setup, following the method developed by Schmid and co-workers [11]. For this measurement, the light transmitted by the reference cavity is divided into two beams (50:50 power split, approx. 70  $\mu$ W): one for cavity mode diagnostics and another for phase noise measurement. The latter is then used for a self-heterodyne-like measurement by performing a beat note with the unmodulated light from the stabilized VECSEL (200  $\mu$ W before the fibre), measured with a balanced photodetector (bandwidth  $\sim 16$  MHz). Figure 3(a) shows the residual fast phase noise measured from the beat note (shown in Fig. 3(b)) for frequencies below the photodetector bandwidth and above 10 kHz (the reference cavity linewidth is  $\sim 5.2$  kHz).

The phase noise starts at a maximum value of  $-126$  dBc/Hz at 10 kHz but remains at values below  $-131$  dBc/Hz for frequencies above 100 kHz, still above the detector noise limit ( $-142$  dBc/Hz). The phase noise increases for frequencies around 3 MHz which might indicate the injection of residual amplitude/frequency modulation by the AOM and/or EOM used for frequency stabilization, which can be further reduced either by the addition of extra feedback electronics to increase correction bandwidth [31] or AOM/EOM temperature stabilization and DC-offset control [32]. The frequency stabilization servo can also contribute to the phase noise peaks measured in this frequency range. The beat note (Fig. 3(b)) has linewidth of 110 Hz with no peak pedestal observed over a 48 MHz range (Fig. 3(b) inset), in-line with previous sub-kHz linewidth results published by our group [20]. Mechanical and thermal noise not completely suppressed by the active stabilization are the main contributors to the phase noise for frequencies below the PZT bandwidth of 30 kHz. The peaks in the 100 kHz to 300 kHz range are generated by the electronics and the pump laser noise, which induces temperature fluctuations in the gain media



that are directly transferred to the VECSEL phase noise [33]. Finally, the total integrated phase noise for the range of frequencies presented here is  $\phi_{\text{RMS}} = 3.2$  mrad.

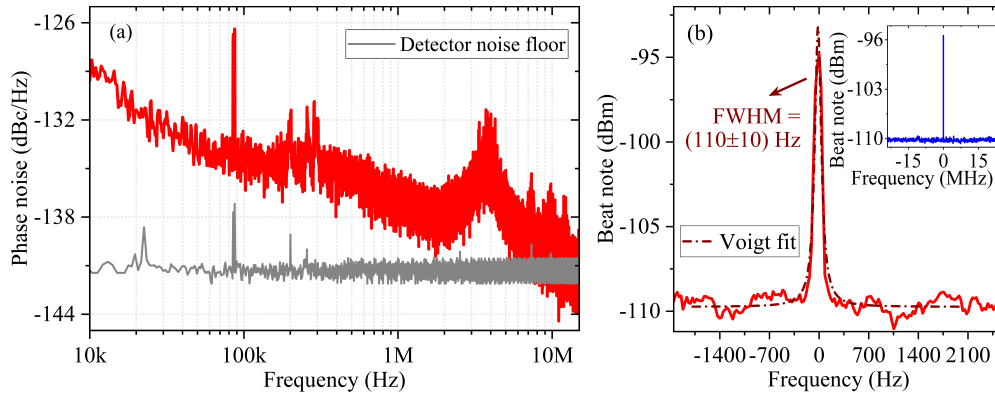


**Fig. 3.** (a) Residual fast phase noise measurements obtained from the beat note between the unmodulated laser light and reference cavity transmission. Measured detector noise is shown in grey. (b) Beat note peak measured using an electrical spectrum analyser and Voigt fit with linewidth of 110 Hz. (inset) beat note peak over a 48 MHz frequency range with no peak pedestal observed.

#### 4. Conclusions

We have developed and characterized the performance of a GaInP/AlGaInP-based VECSEL, frequency-locked at 698 nm, confirming ultra-narrow linewidth (115 Hz) with output power at least an order of magnitude greater than that typically achieved directly from compact lasers at these wavelengths without amplification. Furthermore, we also investigated the residual fast phase noise of a single frequency VECSEL system for the first time using the method developed by Schmid et al. [11], where the phase noise spectrum is calculated via the beat note between the transmission of an ultra-high-finesse cavity and the unmodulated output direct from the laser. The phase noise is less than  $-126$  dBc/Hz for the range of frequencies in this measurement, between 10 kHz and 15 MHz, with a total integrated phase noise of 3.2 mrad. The low phase noise is consistent with previous observations of a pedestal-free beat note measured for a sub-kHz VECSEL using a Hz linewidth, cavity locked laser system [20]. When compared to the measurements of ECDL systems presented in Refs. [4,11], the VECSEL demonstrates residual fast phase noise at least 15 dB lower for frequencies in this measurement range. The total integrated phase noise is also lower, highlighting the advantages of the class-A dynamics characteristic of VECSEL technology.

Miniaturization of the optical pumping scheme, similar to that implemented in our previous work [21], will allow for further reduction of the VECSEL system size, weight, power and costs (SWaP-C). Replacement of the commercial OPSL pump by a high-power laser diode will not only reduce the SWaP-C and complexity of the VECSEL system, but will also enable the implementation of pump intensity stabilization via the diode current, which we have previously used successfully to retain sub-kHz linewidth with the noisier source [21]. The high frequency intensity noise of the pump is filtered out by the high finesse VECSEL. In future work, suppression of the residual amplitude modulation (RAM) in the AOM/EOM [34,35], and increasing the temperature and mechanical stability of the reference cavity, to decrease the influence of environmental noise, can also be implemented. An extended characterization of the phase noise down to mHz frequencies is desired to determine the full impact on the efficiency and

accuracy of quantum technology systems, such as cold atom interferometers [4] used for gravimetry and gradiometer applications. Such low phase noise performance will also enable VECSELs to be used for high precision spectroscopy applications, especially those targeting narrow atomic and molecular transitions at low visible and ultra-violet wavelengths [5]. At these wavelengths, nonlinear frequency conversion techniques are commonly employed which can amplify phase noise from the laser source. The VECSEL low phase noise performance presented in this paper will allow this laser technology to be considered for various high precision applications, including those based on neutral strontium as targeted here.

**Funding.** Engineering and Physical Sciences Research Council (EP/L015315/1, EP/M013294/1, EP/T001046/1).

**Acknowledgements.** The authors thank Erling Riis for lending us the high finesse reference cavity. The laser gain structures were grown by Andrey Krysa at the EPSRC National Centre for III-V Technologies.

**Disclosures.** The authors declare no conflicts of interest.

**Data availability.** Data underlying the results presented in this paper are available in Ref. [36].

## References

1. S. Diehl, A. Micheli, A. Kantian, B. Kraus, H.P. Büchler, and P. Zoller, "Quantum states and phases in driven open quantum systems with cold atoms," *Nat. Phys.* **4**(11), 878–883 (2008).
2. J. Vanier, "Atomic clocks based on coherent population trapping: a review," *Appl. Phys. B* **81**(4), 421–442 (2005).
3. T. Akatsuka, M. Takamoto, and H. Katori, "Optical lattice clocks with non-interacting bosons and fermions," *Nat. Phys.* **4**(12), 954–959 (2008).
4. L. Hu, E.L. Wang, L. Salvi, J.N. Tinsley, G.M. Tino, and N. Poli, "Sr atom interferometry with the optical clock transition as a gravimeter and a gravity gradiometer," *Class. Quantum Grav.* **37**(1), 014001 (2020).
5. N. Kolachevsky, J. Alnis, C.G. Parthey, A. Matveev, R. Landig, and T.W. Hänsch, "Low phase noise diode laser oscillator for 1S–2S spectroscopy in atomic hydrogen," *Opt. Lett.* **36**(21), 4299–4301 (2011).
6. G. Lihachev, J. Riemensberger, W. Weng, J. Liu, H. Tian, A. Siddharth, V. Snigirev, V. Shadymov, A. Voloshin, R.N. Wang, J. He, S.A. Bhave, and T.J. Kippenberg, "Low-noise frequency-agile photonic integrated lasers for coherent ranging," *Nat. Commun.* **13**(1), 3522 (2022).
7. R. Alan, "Distributed optical-fibre sensing," *Meas. Sci. Technol.* **10**(8), R75–R99 (1999).
8. A.L. Schawlow and C.H. Townes, "Infrared and Optical Masers," *Phys. Rev.* **112**(6), 1940–1949 (1958).
9. C.H. Henry, "Theory of the Linewidth of Semiconductor-Lasers," *IEEE J. Quantum Electron.* **18**(2), 259–264 (1982).
10. G. Di Domenico, S. Schilt, and P. Thomann, "Simple approach to the relation between laser frequency noise and laser line shape," *Appl. Opt.* **49**(25), 4801–4807 (2010).
11. F. Schmid, J. Weitenberg, T.W. Hansch, T. Udem, and A. Ozawa, "Simple phase noise measurement scheme for cavity-stabilized laser systems," *Opt. Lett.* **44**(11), 2709–2712 (2019).
12. Y. Zhang, S. Miyakawa, K. Kasai, Y. Okada-Shudo, and M. Watanabe, "Efficient phase noise suppression of an external-cavity diode-laser by optical filtering and resonant optical feedback," *Appl. Phys. B* **108**(1), 39–42 (2012).
13. N. Chauhan, A. Isichenko, K. Liu, J. Wang, Q. Zhao, R.O. Behunin, P.T. Rakich, A.M. Jayich, C. Fertig, C.W. Hoyt, and D.J. Blumenthal, "Visible light photonic integrated Brillouin laser," *Nat. Commun.* **12**(1), 4685 (2021).
14. Z. Xie, W. Liang, A.A. Savchenkov, J. Lim, J. Burkhart, M. McDonald, T. Zhevlevsky, V.S. Ilchenko, A.B. Matsko, L. Maleki, and C.W. Wong, "Extended ultrahigh-Q-cavity diode laser," *Opt. Lett.* **40**(11), 2596–2599 (2015).
15. M. Corato-Zanarella, A. Gil-Molina, X. Ji, M.C. Shin, A. Mohanty, and M. Lipson, "Widely tunable and narrow-linewidth chip-scale lasers from near-ultraviolet to near-infrared wavelengths," *Nat. Photonics* **17**(2), 157–164 (2023).
16. S. Gundavarapu, G.M. Brodnik, M. Puckett, T. Huffman, D. Bose, R. Behunin, J. Wu, T. Qiu, C. Pinho, N. Chauhan, J. Nohava, P.T. Rakich, K.D. Nelson, M. Salit, and D.J. Blumenthal, "Sub-hertz fundamental linewidth photonic integrated Brillouin laser," *Nat. Photonics* **13**(1), 60–67 (2019).
17. M. Guina, A. Rantamaki, and A. Harkonen, "Optically pumped VECSELs: review of technology and progress," *J. Phys. D: Appl. Phys.* **50**(38), 383001 (2017).
18. A.D. Ludlow, M.M. Boyd, J. Ye, E. Peik, and P.O. Schmidt, "Optical atomic clocks," *Rev. Mod. Phys.* **87**(2), 637–701 (2015).
19. R. Le Targat, X. Baillard, M. Fouché, A. Bruschi, O. Tcherbakoff, G.D. Rovera, and P. Lemonde, "Accurate Optical Lattice Clock with  $^{87}\text{Sr}$  Atoms," *Phys. Rev. Lett.* **97**(13), 130801 (2006).
20. P.H. Moriya, Y. Singh, K. Bongs, and J.E. Hastie, "Sub-kHz-linewidth VECSELs for cold atom experiments," *Opt. Express* **28**(11), 15943–15953 (2020).
21. P.H. Moriya, R. Casula, G.A. Chappell, D.C. Parrotta, S. Ranta, H. Kahle, M. Guina, and J.E. Hastie, "InGaN-diode-pumped AlGaInP VECSEL with sub-kHz linewidth at 689 nm," *Opt. Express* **29**(3), 3258–3268 (2021).
22. S. De, A.E. Amili, I. Fsaifes, G. Pillet, G. Baili, F. Goldfarb, M. Alouini, I. Sagnes, and F. Bretenaker, "Phase Noise of the Radio Frequency (RF) Beatnote Generated by a Dual-Frequency VECSEL," *J. Lightwave Technol.* **32**(7), 1307–1316 (2014).

23. S. De, G. Baili, S. Bouchoule, M. Alouini, and F. Bretenaker, "Intensity- and phase-noise correlations in a dual-frequency vertical-external-cavity surface-emitting laser operating at telecom wavelength," *Phys. Rev. A* **91**(5), 053828 (2015).
24. H. Liu, G. Gredat, G. Baili, F. Gutty, F. Goldfarb, I. Sagnes, and F. Bretenaker, "Noise Investigation of a Dual-Frequency VECSEL for Application to Cesium Clocks," *J. Lightwave Technol.* **36**(18), 3882–3891 (2018).
25. G. Gredat, H. Liu, J. Cotxet, F. Tricot, G. Baili, F. Gutty, F. Goldfarb, I. Sagnes, and F. Bretenaker, "Optimization of laser dynamics for active stabilization of DF-VECSELs dedicated to cesium CPT clocks," *J. Opt. Soc. Am. B* **37**(4), 1196–1207 (2020).
26. V.J. Wittwer, R. van der Linden, B.W. Tilma, B. Resan, K.J. Weingarten, T. Sudmeyer, and U. Keller, "Sub-60-fs Timing Jitter of a SESAM Modelocked VECSEL," *IEEE Photonics J.* **5**(1), 1400107 (2013).
27. L. Badurina, E. Bentine, and D. Blas, *et al.*, "AION: an atom interferometer observatory and network," *J. Cosmol. Astropart. Phys.* **2020**(05), 011 (2020).
28. A.J. Kemp, G.J. Valentine, J. Hopkins, J.E. Hastie, S.A. Smith, S. Calvez, M.D. Dawson, and D. Burns, "Thermal management in vertical-external-cavity surface-emitting lasers: finite-element analysis of a heatspreader approach," *IEEE J. Quantum Electron.* **41**(2), 148–155 (2005).
29. D. Paboef and J.E. Hastie, "Tunable narrow linewidth AlGaInP semiconductor disk laser for Sr atom cooling applications," *Appl. Opt.* **55**(19), 4980–4984 (2016).
30. E.D. Black, "An introduction to Pound-Drever-Hall laser frequency stabilization," *Am. J. Phys.* **69**(1), 79–87 (2001).
31. M. Endo and T.R. Schieu, "Residual phase noise suppression for Pound-Drever-Hall cavity stabilization with an electro-optic modulator," *OSA Continuum* **1**(1), 116–123 (2018).
32. Q.A. Duong, T.D. Nguyen, T.T. Vu, M. Higuchi, D. Wei, and M. Aketagawa, "Suppression of residual amplitude modulation appeared in commercial electro-optic modulator to improve iodine-frequency-stabilized laser diode using frequency modulation spectroscopy," *J. Eur. Opt. Soc.-Rapid Publ.* **14**(1), 25 (2018).
33. H. Liu, G. Gredat, S. De, I. Fsaifes, A. Ly, R. Vatr e, G. Baili, S. Bouchoule, F. Goldfarb, and F. Bretenaker, "Ultra-low noise dual-frequency VECSEL at telecom wavelength using fully correlated pumping," *Opt. Lett.* **43**(8), 1794–1797 (2018).
34. E.A. Whittaker, M. Gehrtz, and G.C. Bjorklund, "Residual amplitude modulation in laser electro-optic phase modulation," *J. Opt. Soc. Am. B* **2**(8), 1320–1326 (1985).
35. Y. Yu, Y. Wang, and J.R. Pratt, "Active cancellation of residual amplitude modulation in a frequency-modulation based Fabry-Perot interferometer," *Rev. Sci. Instrum.* **87**(3), 033101 (2016).
36. P.H. Moriya, M. Lee, and J.E. Hastie, *Data for: "Low phase noise operation of a cavity-stabilized 698 nm AlGaInP-based VECSEL"*, University of Strathclyde (2023).